Available online at www.sciencedirect.com
ScienceDirect
Journal of Computational Physics 218 (2006) 594–606
JOURNAL OF COMPUTATIONAL PHYSICS
www.elsevier.com/locate/jcp

Stability of FDTD on nonuniform grids for Maxwell's equations in lossless media

Rob F. Remis *

Delft University of Technology, Faculty of Electrical Engineering, Mathematics and Computer Science, Laboratory of Electromagnetic Research, Mekelweg 4, 2628 CD Delft, ZH, The Netherlands

Received 29 November 2005; received in revised form 22 February 2006; accepted 26 February 2006
Available online 24 April 2006

Abstract

In this paper we present practical stability conditions for the finite-difference time-domain method on nonuniform tensor product grids (Yee grids). These stability conditions apply to Maxwell's equations for inhomogeneous and lossless media. Rectangular domains are considered and the conditions are expressed in terms of the minimum spatial stepsizes of the grid and the maximum electromagnetic wave speed in the configuration. The maximum wave speed is known as soon as the media are specified, while the minimum spatial stepsizes are known after the configuration has been discretized. For two-dimensional configurations we present a number of numerical examples which illustrate the effectiveness of the proposed stability conditions.

MSC: 65M12; 78M20

Keywords: Maxwell's equations; Electromagnetic fields; Finite-difference time-domain; Stability

1. Introduction

The finite-difference time-domain method (FDTD method) is a very popular, explicit and conditionally stable time stepping method for Maxwell's equations. To obtain stable results, the time step Δt has to satisfy the Courant–Friedrichs–Lewy (CFL) stability condition (see [2,4,7,11])

$$\Delta t < 2/\rho(\mathbf{A}), \tag{1}$$

where $\mathbf{A}$ is the first-order Maxwell system matrix and $\rho(\mathbf{A})$ is its spectral radius. The CFL condition is both necessary and sufficient for stability.

The problem with the stability condition of Eq. (1) is that the spectral radius of matrix $\mathbf{A}$ is not known explicitly except for special cases such as uniform grids applied to problems involving homogeneous media (see [2]). In general, we can compute the spectral radius using some iterative eigensolver or we can try to estimate it. The

* Tel.: +31152786050; fax: +31152786194.
E-mail address: R.F.Remis@EWI.TUDelft.NL.

0021-9991/$ - see front matter
doi:10.1016/j.jcp.2006.02.022

first option we like to avoid since it introduces additional computation time to the FDTD solution procedure. The second option is the one we pursue in this paper. Specifically, we determine easily computed upper bounds for the spectral radius of matrix $\mathbf{A}$ in terms of the minimum stepsizes of the grid and the maximum electromagnetic wave speed that is present in the configuration. Denoting these upper bounds by u_k for k-dimensional problems ($k = 1, 2, 3$), we have $\rho(\mathbf{A}) \leqslant u_k$ and we take

$$\Delta t < 2/u_k$$

as a sufficient condition for stability of the FDTD method. Moreover, we also show that for uniform grids and homogeneous media our stability conditions reduce to the well-known conditions that hold for these particular cases. To the knowledge of the author, the stability conditions presented in this paper are not known in the literature.

The paper is organized as follows. In Section 2 we briefly review some aspects of the spatial finite-difference discretization procedure. Most of the material in this section is well known and we only review what is needed in the analysis that follows. The stability analyses for one-, two-, and three-dimensional problems are presented in Sections 3–5, respectively. In Section 6 we present two numerical examples illustrating the effectiveness of the proposed stability condition for two-dimensional configurations.

Finally, we recall some basic facts about matrix norms which are used in the stability analysis that follows. Given a real matrix $\mathbf{C}$, not necessarily square, its maximum column sum norm, spectral norm, and maximum row sum norm are denoted by $\|\mathbf{C}\|_1$, $\|\mathbf{C}\|_2$, and $\|\mathbf{C}\|_\infty$, respectively. For the spectral norm of matrix $\mathbf{C}$ we have the bound

$$\|\mathbf{C}\|_2 \leqslant \sqrt{\|\mathbf{C}\|_1 \|\mathbf{C}\|_\infty}, \tag{2}$$

and if matrix $\mathbf{C}$ is square we also have

$$\rho(\mathbf{C}) \leqslant \|\mathbf{C}\|_2.$$

Equality holds in the latter inequality if $\mathbf{C}$ is normal, that is, if $\mathbf{C}$ commutes with its transpose. Furthermore, the symbol $\otimes$ denotes the Kronecker product (tensor product), the identity matrix of order p is denoted by $\mathbf{I}_p$, and for any matrix $\mathbf{C}$ we have

$$\|\mathbf{I}_p \otimes \mathbf{C}\|_2 = \|\mathbf{C} \otimes \mathbf{I}_q\|_2 = \|\mathbf{C}\|_2. \tag{3}$$

2. Preliminaries

The spatial discretization procedure for Maxwell's equations using two-point finite-difference formulas on staggered nonuniform Cartesian tensor product grids (Yee grids, see [12]) is standard and we only review what is needed to understand the analysis presented in this paper. Much more can be found in [6,10], for example.

We start by normalizing Maxwell's equations with respect to a problem related reference length ℓ. Specifically, we introduce the normalized position vector and normalized time coordinate as $\mathbf{x}' = \ell^{-1}\mathbf{x}$ and $t' = c_0\ell^{-1}t$, respectively, where c_0 is the electromagnetic wave speed in vacuum. In what follows we drop the primes and work with normalized coordinates and field quantities only. Conversion of the stability conditions to the original (unnormalized) coordinates is carried out at the end of the stability analyses for one-, two-, and three-dimensional problems.

The domain of interest is the 3-rectangle

$$\Omega = \{\mathbf{x} \in \mathbb{R}^3; 0 < x < \ell_x, 0 < y < \ell_y, 0 < z < \ell_z\},$$

where $\ell_{x,y,z} > 0$. In this domain an electromagnetic field is present that satisfies the normalized Maxwell's equations

$$-\nabla \times \mathbf{H} + \varepsilon_r \partial_t \mathbf{E} = -\mathbf{J}^{\text{ext}},$$

and

$$\nabla \times \mathbf{E} + \mu_r \partial_t \mathbf{H} = -\mathbf{K}^{\text{ext}},$$

where $\mathbf{J}^{\text{ext}}$ and $\mathbf{K}^{\text{ext}}$ are the known external electric- and magnetic-current densities. These sources start to act at $t = 0$, and no fields are present in Ω prior to this time instant. The time interval of interest is therefore

$$\Omega_T = \{t \in \mathbb{R}; 0 < t < T, T > 0\},$$

and perfect electrically conducting boundary conditions (PEC material boundary conditions) are imposed at the boundary of Ω.

To discretize Maxwell's equations in space, primary and dual grids are introduced in each Cartesian direction. The primary grids in the x-, y-, and z-directions are defined as

$$\Omega_x^{\text{p}} = \{x_p \in \mathbb{R}; p = 0, 1, \ldots, nx + 1, x_p > x_{p-1}, x_0 = 0, x_{nx+1} = \ell_x\},$$
$$\Omega_y^{\text{p}} = \{y_q \in \mathbb{R}; q = 0, 1, \ldots, ny + 1, y_q > y_{q-1}, y_0 = 0, y_{ny+1} = \ell_y\},$$

and

$$\Omega_z^{\text{p}} = \{z_r \in \mathbb{R}; r = 0, 1, \ldots, nz + 1, z_r > z_{r-1}, z_0 = 0, z_{nz+1} = \ell_z\}.$$

The stepsizes of the primary grids are given by $\delta_{x;p} = x_p - x_{p-1}$ for $p = 1, 2, \ldots, nx + 1$, $\delta_{y;q} = y_q - y_{q-1}$ for $q = 1, 2, \ldots, ny + 1$, and $\delta_{z;r} = z_r - z_{r-1}$ for $r = 1, 2, \ldots, nz + 1$. These stepsizes are stored on the diagonal of the stepsize matrices $\mathbf{W}_x$, $\mathbf{W}_y$, and $\mathbf{W}_z$. Specifically

$$\mathbf{W}_x = \text{diag}(\delta_{x;1}, \delta_{x;2}, \ldots, \delta_{x;nx+1}), \quad \mathbf{W}_y = \text{diag}\big(\delta_{y;1}, \delta_{y;2}, \ldots, \delta_{y;ny+1}\big),$$

and

$$\mathbf{W}_z = \text{diag}(\delta_{z;1}, \delta_{z;2}, \ldots, \delta_{z;nz+1}).$$

Moreover, we define the minimum primary stepsizes in the x-, y-, and z-directions as

$$\delta_{x;\min} = \min_p \delta_{x;p}, \quad \delta_{y;\min} = \min_q \delta_{y;q}, \quad \text{and} \quad \delta_{z;\min} = \min_r \delta_{z;r}.$$

The dual grids in the x-, y-, and z-directions are defined as

$$\Omega_x^{\text{d}} = \{\hat{x}_p \in \mathbb{R}; p = 1, 2, \ldots, nx + 1, \hat{x}_{p+1} > \hat{x}_p, 0 < \hat{x}_p < \ell_x\},$$
$$\Omega_y^{\text{d}} = \{\hat{y}_q \in \mathbb{R}; q = 1, 2, \ldots, ny + 1, \hat{y}_{q+1} > \hat{y}_q, 0 < \hat{y}_q < \ell_y\},$$

and

$$\Omega_z^{\text{d}} = \{\hat{z}_r \in \mathbb{R}; r = 1, 2, \ldots, nz + 1, \hat{z}_{r+1} > \hat{z}_r, 0 < \hat{z}_r < \ell_z\},$$

and the stepsizes of the dual grids are given by $\hat{\delta}_{x;p} = \hat{x}_{p+1} - \hat{x}_p$ for $p = 1, 2, \ldots, nx$, $\hat{\delta}_{y;q} = \hat{y}_{q+1} - \hat{y}_q$ for $q = 1, 2, \ldots, ny$, and $\hat{\delta}_{z;r} = \hat{z}_{r+1} - \hat{z}_r$ for $r = 1, 2, \ldots, nz$. All these stepsizes are stored on the diagonal of the stepsize matrices $\widehat{\mathbf{W}}_x$, $\widehat{\mathbf{W}}_y$, and $\widehat{\mathbf{W}}_z$. More precisely, we have

$$\widehat{\mathbf{W}}_x = \text{diag}\Big(\hat{\delta}_{x;1}, \hat{\delta}_{x;2}, \ldots, \hat{\delta}_{x;nx}\Big), \quad \widehat{\mathbf{W}}_y = \text{diag}\Big(\hat{\delta}_{y;1}, \hat{\delta}_{y;2}, \ldots, \hat{\delta}_{y;ny}\Big),$$

and

$$\widehat{\mathbf{W}}_z = \text{diag}\Big(\hat{\delta}_{z;1}, \hat{\delta}_{z;2}, \ldots, \hat{\delta}_{z;nz}\Big).$$

The minimum dual grid stepsizes are defined as

$$\hat{\delta}_{x;\min} = \min_p \hat{\delta}_{x;p}, \quad \hat{\delta}_{y;\min} = \min_q \hat{\delta}_{y;q}, \quad \text{and} \quad \hat{\delta}_{z;\min} = \min_r \hat{\delta}_{z;r}.$$

The purpose of this paper is to present CFL stability conditions in terms of the minimum primary and dual stepsizes and the maximum electromagnetic wave speed.

Since staggered grids are used in almost all FDTD solution strategies, we restrict ourselves to such grids in this paper. Staggered grids are characterized by the property that in each Cartesian direction the dual nodes interlace with the primary nodes. For example, in the x-direction the nodes satisfy

$$0 = x_0 < \hat{x}_1 < x_1 < \hat{x}_2 < \ldots < \hat{x}_{nx+1} < x_{nx+1} = \ell_x. \tag{4}$$

Fig. 1 shows primary and dual nodes in the x-direction with the corresponding stepsizes. At this point we note that a dual node is often placed halfway two primary nodes, that is,

$$\hat{x}_p = \frac{x_p + x_{p-1}}{2} \quad \text{for } p = 1, 2, \ldots, nx+1, \tag{5}$$

see, for example, [6]. In many important applications, however, a dual node is not exactly located in the middle as in Eq. (5). This is the case for optimal grids, for example, as introduced in [1,3]. For an optimal grid it turns out that dual nodes interlace with the primary nodes (as in Eq. (4)), but the nodes do not satisfy Eq. (5). Furthermore, we like to point out that even if Eq. (5) holds then still $\delta_{x;\min} \neq \hat{\delta}_{x;\min}$, in general. For example, with $\ell_x = 1$, $nx = 2$, $\delta_{x;1} = 0.44$, $\delta_{x;2} = 0.12$, $\delta_{x;3} = 0.44$ and Eq. (5), we have $\hat{\delta}_{x;1} = \hat{\delta}_{x;2} = 0.28$ and clearly $\delta_{x;\min} \neq \hat{\delta}_{x;\min}$ in this case. Similar remarks apply to the primary and dual nodes in the y- and z-directions, of course. In what follows we assume that the grid is staggered, but we do not require that a dual node is located halfway two primary nodes.

Having defined the primary and dual grids in the x-, y-, and z-directions, it is customary to introduce Yee cells as

$$\Omega_{\text{Yee};p,q,r} = \{\mathbf{x} \in \mathbb{R}; x_p < x < x_{p+1}, y_q < y < y_{q+1}, z_r < z < z_{r+1}\},$$

for $p = 0, 1, \ldots, nx$, $q = 0, 1, \ldots, ny$, and $r = 0, 1, \ldots, nz$. To comply with the PEC material boundary conditions used for grid termination, the finite difference approximations for the electric field strength are located at the edges of a Yee cell, while the finite difference approximations for the magnetic field strength are located at the faces of a Yee cell (see, again, [6]). For example,

the finite difference approximation of E_x is defined on $\Omega_x^{\mathrm{d}} \times \Omega_y^{\mathrm{p}} \times \Omega_z^{\mathrm{p}} \times \Omega_T$,

and

the finite difference approximation of H_x is defined on $\Omega_x^{\mathrm{p}} \times \Omega_y^{\mathrm{d}} \times \Omega_z^{\mathrm{d}} \times \Omega_T$.

Finally, we introduce two-point differentiation matrices which map finite difference approximations defined on a primary grid in one Cartesian direction to the dual grid in the same direction, and vice versa. Specifically, differentiation of finite-difference approximations defined on the primary grid in the x-direction is carried out by the differentiation matrix

$$\mathbf{X} = -\mathbf{W}_x^{-1}[\text{bidiag}_{nx}(-1, 1)]^{\mathrm{T}},$$

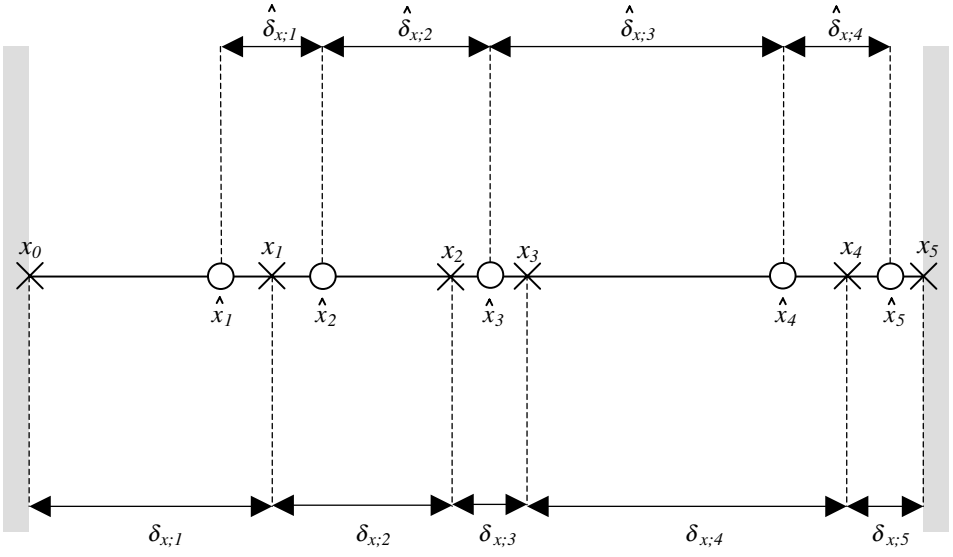

Fig. 1. A one-dimensional staggered grid showing interlacing primary (crosses) and dual (circles) nodes ($nx = 4$).

while differentiation of finite-difference approximations defined on the dual grid in the x-direction is carried out by

$$\widehat{\mathbf{X}} = \widehat{\mathbf{W}}_x^{-1}\text{bidiag}_{nx}(-1,1).$$

In the above expressions, $\text{bidiag}_{nx}(-1,1)$ is nx-by-$(nx+1)$ and upper bidiagonal with -1 on the diagonal and $+1$ on the upper diagonal. Similarly, we have

$$\mathbf{Y} = -\mathbf{W}_y^{-1}[\text{bidiag}_{ny}(-1,1)]^{\mathrm{T}}, \quad \widehat{\mathbf{Y}} = \widehat{\mathbf{W}}_y^{-1}\text{bidiag}_{ny}(-1,1),$$
$$\mathbf{Z} = -\mathbf{W}_z^{-1}[\text{bidiag}_{nz}(-1,1)]^{\mathrm{T}}, \quad \text{and} \quad \widehat{\mathbf{Z}} = \widehat{\mathbf{W}}_z^{-1}\text{bidiag}_{nz}(-1,1).$$

These matrices are nonsquare and in what follows we need upper bounds for the spectral norms of these matrices. Using Eq. (2), it is easily verified that

$$\|\mathbf{X}\|_2 \leqslant \frac{2}{\delta_{x;\min}}, \quad \|\mathbf{Y}\|_2 \leqslant \frac{2}{\delta_{y;\min}}, \quad \|\mathbf{Z}\|_2 \leqslant \frac{2}{\delta_{z;\min}}, \tag{6}$$

and

$$\|\widehat{\mathbf{X}}\|_2 \leqslant \frac{2}{\hat{\delta}_{x;\min}}, \quad \|\widehat{\mathbf{Y}}\|_2 \leqslant \frac{2}{\hat{\delta}_{y;\min}}, \quad \|\widehat{\mathbf{Z}}\|_2 \leqslant \frac{2}{\hat{\delta}_{z;\min}}. \tag{7}$$

After the spatial discretization procedure one arrives for one-, two-, and three-dimensional problems at the so-called finite-difference state-space representation (see [2]):

$$(\mathbf{D} + \mathbf{M}\partial_t)\mathbf{f} = -\mathbf{q}, \tag{8}$$

where matrix $\mathbf{D}$ is the spatial differentiation matrix, $\mathbf{M}$ is a diagonal and positive definite medium matrix with relative permittivity and permeability values on the diagonal, $\mathbf{f}$ is the field vector containing the finite-difference approximations, and $\mathbf{q}$ is the source vector. The smallest relative permittivity value on the grid is denoted by $\varepsilon_{\mathrm{r};\min}$ and the smallest relative permeability value by $\mu_{\mathrm{r};\min}$. Explicit expressions for the differentiation matrix $\mathbf{D}$ and the medium matrix $\mathbf{M}$ are given in the sections below.

The state-space representation of Eq. (8) can be rewritten in terms of the so-called system matrix

$$\mathbf{A} = \mathbf{M}^{-1/2}\mathbf{D}\mathbf{M}^{-1/2} \tag{9}$$

as

$$(\mathbf{A} + \mathbf{I}_n\partial_t)\tilde{\mathbf{f}} = -\tilde{\mathbf{q}},$$

where n is the order of the system, and the scaled field and source vector are given by

$$\tilde{\mathbf{f}} = \mathbf{M}^{1/2}\mathbf{f} \quad \text{and} \quad \tilde{\mathbf{q}} = \mathbf{M}^{-1/2}\mathbf{q},$$

respectively. Now in the FDTD method, the time coordinate in Eq. (8) is discretized in a leap-frog manner using a time step Δt. To obtain stable results, this time step has to satisfy the CFL condition of Eq. (1), where matrix $\mathbf{A}$ is given by Eq. (9). We take this condition as a starting point and follow the procedure outlined in the previous section to obtain explicit stability conditions for one-, two-, and three-dimensional problems.

3. One-dimensional problems

We consider a one-dimensional configuration with no variation in the x- and z-directions. For this problem the differentiation matrix $\mathbf{D}$ and the medium matrix $\mathbf{M}$ can be written as

$$\mathbf{D} = \begin{pmatrix} 0 & \widehat{\mathbf{Y}} \\ \mathbf{Y} & 0 \end{pmatrix} \quad \text{and} \quad \mathbf{M} = \begin{pmatrix} \mathbf{M}_\varepsilon & 0 \\ 0 & \mathbf{M}_\mu \end{pmatrix}.$$

The matrices $\mathbf{M}_\varepsilon$ and $\mathbf{M}_\mu$ are both diagonal and positive definite with relative permittivity and permeability values on the diagonal. The system matrix for this particular problem is given by

$$\mathbf{A} = \begin{pmatrix} 0 & \mathbf{A}_1 \\ \mathbf{A}_2 & 0 \end{pmatrix},$$

where

$$\mathbf{A}_1 = \mathbf{M}_\varepsilon^{-1/2}\widehat{\mathbf{Y}}\mathbf{M}_\mu^{-1/2} \quad \text{and} \quad \mathbf{A}_2 = \mathbf{M}_\mu^{-1/2}\mathbf{Y}\mathbf{M}_\varepsilon^{-1/2}.$$

To find an upper bound for the spectral radius of matrix $\mathbf{A}$, we start by considering the eigenvalue problem

$$\mathbf{A}\mathbf{x} = \lambda\mathbf{x} \quad (\mathbf{x} \neq \mathbf{0}).$$

Partitioning the eigenvector $\mathbf{x}$ conform the partitioning of matrix $\mathbf{A}$ as $\mathbf{x} = (\mathbf{x}_\mathrm{e}^\mathrm{T}, \mathbf{x}_\mathrm{h}^\mathrm{T})^\mathrm{T}$, we obtain

$$\mathbf{A}_1\mathbf{x}_\mathrm{h} = \lambda\mathbf{x}_\mathrm{e} \quad \text{and} \quad \mathbf{A}_2\mathbf{x}_\mathrm{e} = \lambda\mathbf{x}_\mathrm{h}.$$

For nonzero eigenvalues we can eliminate $\mathbf{x}_\mathrm{h}$ from the above two equations. We obtain

$$\mathbf{A}_1\mathbf{A}_2\mathbf{x}_\mathrm{e} = \lambda^2\mathbf{x}_\mathrm{e},$$

from which we conclude that

$$\rho(\mathbf{A}) = \sqrt{\rho(\mathbf{A}_1\mathbf{A}_2)}.$$

Furthermore, since $\rho(\mathbf{A}_1\mathbf{A}_2) \leqslant \|\mathbf{A}_1\|_2\|\mathbf{A}_2\|_2$ we have

$$\rho(\mathbf{A}) \leqslant \sqrt{\|\mathbf{A}_1\|_2\|\mathbf{A}_2\|_2}, \tag{10}$$

and for the spectral norms of $\mathbf{A}_1$ and $\mathbf{A}_2$ we have the bounds

$$\|\mathbf{A}_1\|_2 \leqslant \frac{1}{\sqrt{\varepsilon_{\mathrm{r;min}}\mu_{\mathrm{r;min}}}}\frac{2}{\hat{\delta}_{y;\mathrm{min}}} \quad \text{and} \quad \|\mathbf{A}_2\|_2 \leqslant \frac{1}{\sqrt{\varepsilon_{\mathrm{r;min}}\mu_{\mathrm{r;min}}}}\frac{2}{\delta_{y;\mathrm{min}}},$$

where we have used the relevant inequalities of Eqs. (6) and (7). From the above two bounds and Eq. (10) it follows that

$$\rho(\mathbf{A}) \leqslant \frac{2}{\sqrt{\varepsilon_{\mathrm{r;min}}\mu_{\mathrm{r;min}}}}\frac{1}{\sqrt{\delta_{y;\mathrm{min}}\hat{\delta}_{y;\mathrm{min}}}} =: u_1.$$

This leads to the stability condition

$$\Delta t' < \sqrt{\varepsilon_{\mathrm{r;min}}\mu_{\mathrm{r;min}}}\sqrt{\delta'_{y;\mathrm{min}}\hat{\delta}'_{y;\mathrm{min}}},$$

where we have introduced the primes again to indicate that we are dealing with normalized stepsizes. The stability condition for the unnormalized stepsizes follows by multiplying the above inequality by $c_0^{-1}\ell$. We obtain

$$\Delta t < \frac{1}{c_\mathrm{max}}\sqrt{\delta_{y;\mathrm{min}}\hat{\delta}_{y;\mathrm{min}}}, \tag{11}$$

where

$$c_\mathrm{max} = \frac{1}{\sqrt{\varepsilon_0\varepsilon_{\mathrm{r;min}}\mu_0\mu_{\mathrm{r;min}}}}$$

is the maximum electromagnetic wave speed. Notice that for a uniform grid with stepsize δ the above stability condition simplifies to the well-known result

$$\Delta t < \frac{\delta}{c_\mathrm{max}}.$$

4. Two-dimensional problems

For two-dimensional problems (no variation in the z-direction) we consider E-polarized fields only, since the analysis for H-polarized fields is very similar.

Using Kronecker product notation, the spatial differentiation matrix can be written in the form (see [8])

$$\mathbf{D} = \begin{pmatrix} 0 & \mathbf{Y} \otimes \mathbf{I}_{nx} & 0 \\ \widehat{\mathbf{Y}} \otimes \mathbf{I}_{nx} & 0 & -\mathbf{I}_{ny} \otimes \widehat{\mathbf{X}} \\ 0 & -\mathbf{I}_{ny} \otimes \mathbf{X} & 0 \end{pmatrix},$$

and the medium matrix $\mathbf{M}$ is given by

$$\mathbf{M} = \begin{pmatrix} \mathbf{M}_{\mu;x} & 0 & 0 \\ 0 & \mathbf{M}_{\varepsilon} & 0 \\ 0 & 0 & \mathbf{M}_{\mu;y} \end{pmatrix}.$$

Again, matrix $\mathbf{M}$ is diagonal and positive definite. Also note that $\mathbf{M}_{\mu;x}$ is different from $\mathbf{M}_{\mu;y}$, since $\mathbf{M}_{\mu;x}$ contains (averaged) permeability values at locations where the finite difference approximation for H_x is defined, while $\mathbf{M}_{\mu;y}$ contains permeability values at locations where finite difference approximations for H_y are defined. Furthermore, the system matrix is given by

$$\mathbf{A} = \begin{pmatrix} 0 & \mathbf{A}_1 & 0 \\ \mathbf{A}_2 & 0 & \mathbf{A}_3 \\ 0 & \mathbf{A}_4 & 0 \end{pmatrix},$$

with

$$\mathbf{A}_1 = \mathbf{M}_{\mu;x}^{-1/2}(\mathbf{Y} \otimes \mathbf{I}_{nx})\mathbf{M}_{\varepsilon}^{-1/2}, \quad \mathbf{A}_2 = \mathbf{M}_{\varepsilon}^{-1/2}\left(\widehat{\mathbf{Y}} \otimes \mathbf{I}_{nx}\right)\mathbf{M}_{\mu;x}^{-1/2},$$
$$\mathbf{A}_3 = -\mathbf{M}_{\varepsilon}^{-1/2}(\mathbf{I}_{ny} \otimes \widehat{\mathbf{X}})\mathbf{M}_{\mu;y}^{-1/2}, \quad \text{and} \quad \mathbf{A}_4 = -\mathbf{M}_{\mu;y}^{-1/2}(\mathbf{I}_{ny} \otimes \mathbf{X})\mathbf{M}_{\varepsilon}^{-1/2}.$$

Consider again the eigenvalue problem for matrix $\mathbf{A}$ and partition the eigenvector $\mathbf{x}$ conform the partitioning of matrix $\mathbf{A}$ as $\mathbf{x} = (\mathbf{x}_{\mathrm{h}x}^{\mathrm{T}}, \mathbf{x}_{\mathrm{e}z}^{\mathrm{T}}, \mathbf{x}_{\mathrm{h}y}^{\mathrm{T}})^{\mathrm{T}}$. For nonzero eigenvalues we can eliminate $\mathbf{x}_{\mathrm{h}x}$ and $\mathbf{x}_{\mathrm{h}y}$ from the eigensystem to obtain

$$(\mathbf{A}_2\mathbf{A}_1 + \mathbf{A}_3\mathbf{A}_4)\mathbf{x}_{\mathrm{e}z} = \lambda^2\mathbf{x}_{\mathrm{e}z}$$

from which we observe that

$$\rho(\mathbf{A}) = \sqrt{\rho(\mathbf{A}_2\mathbf{A}_1 + \mathbf{A}_3\mathbf{A}_4)}.$$

Moreover, since

$$\rho(\mathbf{A}_2\mathbf{A}_1 + \mathbf{A}_3\mathbf{A}_4) \leqslant \|\mathbf{A}_1\|_2\|\mathbf{A}_2\|_2 + \|\mathbf{A}_3\|_2\|\mathbf{A}_4\|_2$$

we get

$$\rho(\mathbf{A}) \leqslant \sqrt{\|\mathbf{A}_1\|_2\|\mathbf{A}_2\|_2 + \|\mathbf{A}_3\|_2\|\mathbf{A}_4\|_2}.$$

For the spectral norms of $\mathbf{A}_1$, $\mathbf{A}_2$, $\mathbf{A}_3$, and $\mathbf{A}_4$ we have the bounds

$$\|\mathbf{A}_1\|_2 \leqslant \frac{1}{\sqrt{\varepsilon_{\mathrm{r;min}}\mu_{\mathrm{r;min}}}}\frac{2}{\delta_{y;\min}}, \quad \|\mathbf{A}_2\|_2 \leqslant \frac{1}{\sqrt{\varepsilon_{\mathrm{r;min}}\mu_{\mathrm{r;min}}}}\frac{2}{\hat{\delta}_{y;\min}},$$
$$\|\mathbf{A}_3\|_2 \leqslant \frac{1}{\sqrt{\varepsilon_{\mathrm{r;min}}\mu_{\mathrm{r;min}}}}\frac{2}{\hat{\delta}_{x;\min}}, \quad \text{and} \quad \|\mathbf{A}_4\|_2 \leqslant \frac{1}{\sqrt{\varepsilon_{\mathrm{r;min}}\mu_{\mathrm{r;min}}}}\frac{2}{\delta_{x;\min}},$$

where we have used Eqs. (3), (6) and (7). Putting everything together, we arrive at

$$\rho(\mathbf{A}) \leqslant \frac{2}{\sqrt{\varepsilon_{\mathrm{r;min}}\mu_{\mathrm{r;min}}}} \sqrt{\frac{\delta_{x;\min}\hat{\delta}_{x;\min} + \delta_{y;\min}\hat{\delta}_{y;\min}}{\delta_{x;\min}\hat{\delta}_{x;\min}\delta_{y;\min}\hat{\delta}_{y;\min}}} =: u_2$$

and this leads to the stability condition for unnormalized stepsizes

$$\Delta t < \frac{1}{c_{\max}} \sqrt{\frac{\delta_{x;\min}\hat{\delta}_{x;\min}\delta_{y;\min}\hat{\delta}_{y;\min}}{\delta_{x;\min}\hat{\delta}_{x;\min} + \delta_{y;\min}\hat{\delta}_{y;\min}}}. \tag{12}$$

For a uniform grid with stepsize δ_x in the x-direction and stepsize δ_y in the y-direction, the above bound simplifies to

$$\Delta t < \frac{1}{c_{\max}} \frac{1}{\sqrt{\frac{1}{\delta_x^2} + \frac{1}{\delta_y^2}}}$$

and if, in addition, $\delta_x = \delta_y = \delta$, we get

$$\Delta t < \frac{\delta}{\sqrt{2}c_{\max}}.$$

5. Three-dimensional problems

For three-dimensional problems, the differentiation matrix can be written in the form (see [2] for uniform grids)

$$\mathbf{D} = \begin{pmatrix} 0 & \mathbf{D}_{\mathrm{h}} \\ \mathbf{D}_{\mathrm{e}} & 0 \end{pmatrix},$$

where $\mathbf{D}_{\mathrm{h}}$ is a differentiation matrix operating on the magnetic field strength approximations and is given by

$$\mathbf{D}_{\mathrm{h}} = \begin{pmatrix} 0 & \widehat{\mathbf{Z}} \otimes \mathbf{I}_{ny} \otimes \mathbf{I}_{nx+1} & -\mathbf{I}_{nz} \otimes \widehat{\mathbf{Y}} \otimes \mathbf{I}_{nx+1} \\ -\widehat{\mathbf{Z}} \otimes \mathbf{I}_{ny+1} \otimes \mathbf{I}_{nx} & 0 & \mathbf{I}_{nz} \otimes \mathbf{I}_{ny+1} \otimes \widehat{\mathbf{X}} \\ \mathbf{I}_{nz+1} \otimes \widehat{\mathbf{Y}} \otimes \mathbf{I}_{nx} & -\mathbf{I}_{nz+1} \otimes \mathbf{I}_{ny} \otimes \widehat{\mathbf{X}} & 0 \end{pmatrix},$$

while $\mathbf{D}_{\mathrm{e}}$ differentiates electric field strength approximations and is given by

$$\mathbf{D}_{\mathrm{e}} = \begin{pmatrix} 0 & -\mathbf{Z} \otimes \mathbf{I}_{ny+1} \otimes \mathbf{I}_{nx} & \mathbf{I}_{nz+1} \otimes \mathbf{Y} \otimes \mathbf{I}_{nx} \\ \mathbf{Z} \otimes \mathbf{I}_{ny} \otimes \mathbf{I}_{nx+1} & 0 & -\mathbf{I}_{nz+1} \otimes \mathbf{I}_{ny} \otimes \mathbf{X} \\ -\mathbf{I}_{nz} \otimes \mathbf{Y} \otimes \mathbf{I}_{nx+1} & \mathbf{I}_{nz} \otimes \mathbf{I}_{ny+1} \otimes \mathbf{X} & 0 \end{pmatrix}.$$

Furthermore, the medium matrix is given by

$$\mathbf{M} = \begin{pmatrix} \mathbf{M}_{\varepsilon} & 0 \\ 0 & \mathbf{M}_{\mu} \end{pmatrix}$$

and this matrix is diagonal and positive definite. Finally, the system matrix for three-dimensional problems is

$$\mathbf{A} = \begin{pmatrix} 0 & \mathbf{A}_1 \\ \mathbf{A}_2 & 0 \end{pmatrix},$$

where

$$\mathbf{A}_1 = \mathbf{M}_{\varepsilon}^{-1/2}\mathbf{D}_{\mathrm{h}}\mathbf{M}_{\mu}^{-1/2} \quad \text{and} \quad \mathbf{A}_2 = \mathbf{M}_{\mu}^{-1/2}\mathbf{D}_{\mathrm{e}}\mathbf{M}_{\varepsilon}^{-1/2}.$$

We observe that this matrix is similar in form as the system matrix for one-dimensional problems. Consequently, the stability analysis is very similar to the analysis of one-dimensional problems. We do need bounds for the spectral norms of the differentiation matrices $\mathbf{D}_{\mathrm{h}}$ and $\mathbf{D}_{\mathrm{e}}$ to carry out this analysis. These bounds are provided by the following lemma.

Lemma 1. *For the spectral norms of the differentiation matrices* $\mathbf{D}_h$ *and* $\mathbf{D}_e$ *we have the following bounds*:

$$\|\mathbf{D}_\mathrm{h}\|_2 \leqslant 2\sqrt{\frac{1}{\hat{\delta}^2_{x;\min}}+\frac{1}{\hat{\delta}^2_{y;\min}}+\frac{1}{\hat{\delta}^2_{z;\min}}}, \tag{13}$$

and

$$\|\mathbf{D}_\mathrm{e}\|_2 \leqslant 2\sqrt{\frac{1}{\delta^2_{x;\min}}+\frac{1}{\delta^2_{y;\min}}+\frac{1}{\delta^2_{z;\min}}}. \tag{14}$$

Proof. We only proof the first bound, since the second one can be obtained by following similar steps.

The spectral norm of matrix $\mathbf{D}_\mathrm{h}$ is equal to its largest singular value. Denoting this singular value by σ_1, we have

$$\mathbf{D}_\mathrm{h}\mathbf{D}_\mathrm{h}^\mathrm{T}\mathbf{u}_1 = \sigma_1^2\mathbf{u}_1, \tag{15}$$

where $\mathbf{u}_1$ is a left singular vector corresponding to σ_1. Introducing the divergence operator $\mathbf{N}_\mathrm{e}$ as

$$\mathbf{N}_\mathrm{e} = \begin{pmatrix} \mathbf{I}_{nz}\otimes\mathbf{I}_{ny}\otimes\widehat{\mathbf{X}} & \mathbf{I}_{nz}\otimes\widehat{\mathbf{Y}}\otimes\mathbf{I}_{nx} & \widehat{\mathbf{Z}}\otimes\mathbf{I}_{ny}\otimes\mathbf{I}_{nx}\end{pmatrix}$$

it is easily verified that

$$\mathbf{N}_\mathrm{e}\mathbf{D}_\mathrm{h} = \mathbf{0}. \tag{16}$$

Applying the divergence operator to Eq. (15) and using Eq. (16), we obtain

$$\mathbf{N}_\mathrm{e}\mathbf{u}_1 = \mathbf{0}. \tag{17}$$

This shows that the left singular vector is divergence-free. Subsequently, we write the product $\mathbf{D}_\mathrm{h}\mathbf{D}_\mathrm{h}^\mathrm{T}$ out in full. We obtain

$$\mathbf{D}_\mathrm{h}\mathbf{D}_\mathrm{h}^\mathrm{T} = \mathbf{L} - \mathbf{G}_\mathrm{h}\begin{pmatrix}\mathbf{N}_\mathrm{e}\\ \mathbf{N}_\mathrm{e}\\ \mathbf{N}_\mathrm{e}\end{pmatrix}, \tag{18}$$

where $\mathbf{G}_\mathrm{h}$ is the gradient operator given by

$$\mathbf{G}_\mathrm{h} = \begin{pmatrix} \mathbf{I}_{nz}\otimes\mathbf{I}_{ny}\otimes\widehat{\mathbf{X}}^\mathrm{T} & 0 & 0\\ 0 & \mathbf{I}_{nz}\otimes\widehat{\mathbf{Y}}^\mathrm{T}\otimes\mathbf{I}_{nx} & 0\\ 0 & 0 & \widehat{\mathbf{Z}}^\mathrm{T}\otimes\mathbf{I}_{ny}\otimes\mathbf{I}_{nx}\end{pmatrix},$$

and matrix $\mathbf{L}$ is given by

$$\mathbf{L} = \begin{pmatrix}\mathbf{L}_{\mathrm{h}x} & 0 & 0\\ 0 & \mathbf{L}_{\mathrm{h}y} & 0\\ 0 & 0 & \mathbf{L}_{\mathrm{h}z}\end{pmatrix},$$

with

$$\mathbf{L}_{\mathrm{h}x} = \left(\widehat{\mathbf{Z}}\widehat{\mathbf{Z}}^\mathrm{T}\right)\otimes\mathbf{I}_{ny}\otimes\mathbf{I}_{nx+1} + \mathbf{I}_{nz}\otimes\left(\widehat{\mathbf{Y}}\widehat{\mathbf{Y}}^\mathrm{T}\right)\otimes\mathbf{I}_{nx+1} + \mathbf{I}_{nz}\otimes\mathbf{I}_{ny}\otimes\left(\widehat{\mathbf{X}}^\mathrm{T}\widehat{\mathbf{X}}\right),$$
$$\mathbf{L}_{\mathrm{h}y} = \left(\widehat{\mathbf{Z}}\widehat{\mathbf{Z}}^\mathrm{T}\right)\otimes\mathbf{I}_{ny+1}\otimes\mathbf{I}_{nx} + \mathbf{I}_{nz}\otimes\left(\widehat{\mathbf{Y}}^\mathrm{T}\widehat{\mathbf{Y}}\right)\otimes\mathbf{I}_{nx} + \mathbf{I}_{nz}\otimes\mathbf{I}_{ny+1}\otimes\left(\widehat{\mathbf{X}}\widehat{\mathbf{X}}^\mathrm{T}\right),$$

and

$$\mathbf{L}_{\mathrm{h}z} = \left(\widehat{\mathbf{Z}}^\mathrm{T}\widehat{\mathbf{Z}}\right)\otimes\mathbf{I}_{ny}\otimes\mathbf{I}_{nx} + \mathbf{I}_{nz+1}\otimes\left(\widehat{\mathbf{Y}}\widehat{\mathbf{Y}}^\mathrm{T}\right)\otimes\mathbf{I}_{nx} + \mathbf{I}_{nz+1}\otimes\mathbf{I}_{ny}\otimes\left(\widehat{\mathbf{X}}\widehat{\mathbf{X}}^\mathrm{T}\right).$$

Notice that $\mathbf{L}_{\mathrm{h}x}$, $\mathbf{L}_{\mathrm{h}y}$, and $\mathbf{L}_{\mathrm{h}z}$ are real and symmetric matrices, and

$$\rho(\mathbf{L}_{\mathrm{hx}}) = \rho(\mathbf{L}_{\mathrm{hy}}) = \rho(\mathbf{L}_{\mathrm{hz}}). \tag{19}$$

Substituting Eq. (18) in Eq. (15) and using Eq. (17), we obtain

$$\mathbf{L}\mathbf{u}_1 = \sigma_1^2 \mathbf{u}_1$$

from which we conclude that

$$\|\mathbf{D}_{\mathrm{h}}\|_2 = \sigma_1 = \sqrt{\rho(\mathbf{L})}.$$

Given the expression for matrix $\mathbf{L}$ and because of Eq. (19) we have

$$\rho(\mathbf{L}) = \rho(\mathbf{L}_{\mathrm{hx}}) = \rho(\mathbf{L}_{\mathrm{hy}}) = \rho(\mathbf{L}_{\mathrm{hz}}).$$

Taking the spectral radius of matrix $\mathbf{L}_{\mathrm{h}x}$ (taking one of the other spectral radii leads to the same result) and using the fact that $\mathbf{L}_{\mathrm{h}x}$ is symmetric, we obtain

$$\rho(\mathbf{L}) = \rho(\mathbf{L}_{\mathrm{hx}}) = \|\mathbf{L}_{\mathrm{hx}}\|_2.$$

Finally, with the help of Eqs. (3), (6) and (7) we arrive at the bound

$$\|\mathbf{L}_{\mathrm{hx}}\|_2 \leqslant 4\left(\frac{1}{\hat{\delta}^2_{x;\min}} + \frac{1}{\hat{\delta}^2_{y;\min}} + \frac{1}{\hat{\delta}^2_{z;\min}}\right)$$

and the result follows. □

As stated above, we can now obtain a stability bound for 3D problems by following essentially the same steps as for 1D problems. For the spectral radius of matrix $\mathbf{A}$ we have

$$\rho(\mathbf{A}) = \sqrt{\rho(\mathbf{A}_1\mathbf{A}_2)} \leqslant \sqrt{\|\mathbf{A}_1\|_2\|\mathbf{A}_2\|_2},$$

and for the spectral norms of $\mathbf{A}_1$ and $\mathbf{A}_2$ we obtain

$$\|\mathbf{A}_1\|_2 \leqslant \frac{1}{\sqrt{\varepsilon_{\mathrm{r};\min}\mu_{\mathrm{r};\min}}}\|\mathbf{D}_{\mathrm{h}}\|_2 \quad \text{and} \quad \|\mathbf{A}_2\|_2 \leqslant \frac{1}{\sqrt{\varepsilon_{\mathrm{r};\min}\mu_{\mathrm{r};\min}}}\|\mathbf{D}_{\mathrm{e}}\|_2.$$

Combining these bounds with the bounds of the lemma results in

$$\rho(\mathbf{A}) \leqslant \frac{2}{\sqrt{\varepsilon_{\mathrm{r};\min}\mu_{\mathrm{r};\min}}}\left(\frac{1}{\delta^2_{x;\min}} + \frac{1}{\delta^2_{y;\min}} + \frac{1}{\delta^2_{z;\min}}\right)^{1/4}\left(\frac{1}{\hat{\delta}^2_{x;\min}} + \frac{1}{\hat{\delta}^2_{y;\min}} + \frac{1}{\hat{\delta}^2_{z;\min}}\right)^{1/4} =: u_3,$$

and this leads to the stability condition

$$\Delta t < \frac{1}{c_{\max}} \frac{1}{\left(\frac{1}{\delta^2_{x;\min}} + \frac{1}{\delta^2_{y;\min}} + \frac{1}{\delta^2_{z;\min}}\right)^{1/4}\left(\frac{1}{\hat{\delta}^2_{x;\min}} + \frac{1}{\hat{\delta}^2_{y;\min}} + \frac{1}{\hat{\delta}^2_{z;\min}}\right)^{1/4}}. \tag{20}$$

For a uniform grid with stepsize δ_x in the x-direction, δ_y in the y-direction, and δ_z in the z-direction, we get

$$\Delta t < \frac{1}{c_{\max}} \frac{1}{\sqrt{\frac{1}{\delta_x^2} + \frac{1}{\delta_y^2} + \frac{1}{\delta_z^2}}},$$

and if, in addition, $\delta_x = \delta_y = \delta_z = \delta$, this becomes

$$\Delta t < \frac{\delta}{\sqrt{3}c_{\max}}.$$

6. Numerical examples

To show the effectiveness of the upper bounds proposed in this paper, we have carried out two numerical experiments for two-dimensional E-polarized electromagnetic fields. In both experiments homogeneous blocks

are present in a vacuum domain. These blocks have dielectric contrast only, that is, the permittivity differs from ε_0 and the permeability of the blocks equals that of vacuum.

In the examples the spatial discretization was chosen to accurately describe the propagation of electromagnetic waves as generated by an external electric-current source with the derivative of a Gaussian pulse as a source wavelet. The peak frequency of this wavelet was taken as $f_{\text{peak}} = 900$ MHz. To this frequency there corresponds a wavelength $\lambda = c/f_{\text{peak}}$ and the spatial stepsizes were chosen such that we have at least 33 points per λ everywhere in the computational domain. In both examples, the dual nodes interlace with the primary nodes and a dual node is always placed halfway two primary nodes.

To measure the effectiveness of our stability condition we introduce a reduction factor α as

$$\alpha = \rho(\mathbf{A})/u_2.$$

Clearly, $0 < \alpha \leqslant 1$ and if u_2 is close to $\rho(\mathbf{A})$ then α is close to one. The reason for calling α a reduction factor is that if we take $\Delta t = 2/u_2$ as the time step in FDTD, then

$$\Delta t = \alpha \frac{2}{\rho(\mathbf{A})}.$$

This shows that the larger α is, the closer we are to the CFL upper limit $2/\rho(\mathbf{A})$.

In our first example we consider a square block of $2\lambda_0$-by-$2\lambda_0$ (λ_0 is the wavelength in vacuum that corresponds to the peak frequency) located in a vacuum domain. The block has a relative permittivity $\varepsilon_r = 4$ and is centered in the middle of the total computational domain of $6\lambda_0$-by-$6\lambda_0$. Since the wavelength shrinks by a factor of two inside the block, we have halved the stepsizes in and around the block. Fig. 2 shows a detail of the complete configuration. The total number of unknowns for this problem is 208,033.

The spectral radius of matrix $\mathbf{A}$ was computed using ARPACK [5] and was found to be $\rho(\mathbf{A}) = 1.086783 \times 10^3$. Our upper bound produces $u_2 = 1.120058 \times 10^3$ leading to a reduction factor of $\alpha \approx 0.97$. In other words, the upper bound is fairly close to the true upper bound in this case.

Our second example is taken from [9]. Two small square blocks both with a relative permittivity $\varepsilon_r = 64$ are located in a vacuum domain. Part of the configuration is shown in Fig. 3. The blocks are located at the centers of the "plus-signs". These signs appear due to grid refinement and as a consequence the blocks are not visible in Fig. 3. We therefore show a more detailed part of the configuration in Fig. 4. The total configuration is $6\lambda_0$-by-$6\lambda_0$ and the side length of the blocks is $\lambda_0/100$. Furthermore, the stepsizes are halved as we approach the blocks along each Cartesian direction. After the cell size has been reduced by a factor of two, we keep the stepsize fixed for two cells and then repeat the process until 10 stepsizes make up the side length of the small block in each Cartesian direction (see also Fig. 4). The total number of unknowns for this problem is 152,995 and again we computed the spectral radius of matrix $\mathbf{A}$ using ARPACK. The spectral radius was found to be $\rho(\mathbf{A}) = 1.617291 \times 10^4$ and our upper bound produces $u_2 = 1.796575 \times 10^4$ resulting in a reduction factor

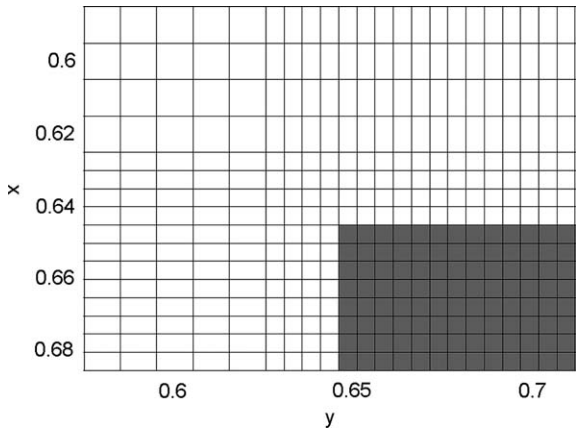

Fig. 2. Detail of the computational domain showing grid refinement and nonuniform Yee cells. The upper left corner of the block is seen in the lower right corner of the figure. The relative permittivity of the block is $\varepsilon_r = 4$ and it is located in vacuum.

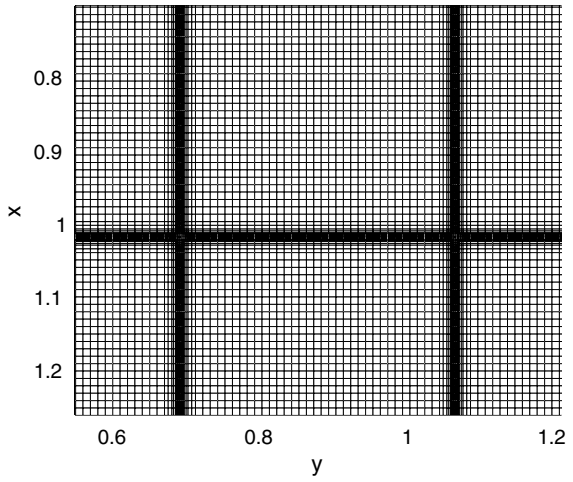

Fig. 3. Detail of the computational domain showing grid refinement for the second example. Two small blocks both with a relative permittivity $\varepsilon_r = 64$ located in vacuum. The blocks are located at the centers of the "plus signs" and are not visible due to grid refinement.

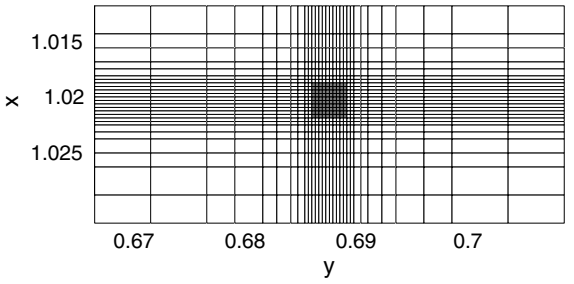

Fig. 4. Detail of the computational domain showing grid refinement, nonuniform Yee cells, and one of the blocks with a relative permittivity $\varepsilon_r = 64$.

$\alpha \approx 0.90$. This result is not as good as the result of the previous example, but the upper bound is still fairly close to the CFL limit in this case.

This immediately brings us to the question whether the estimates presented in this paper are sharp or not. Although we do not have a proof, we expect that the bounds are fairly sharp for problems encountered in practice. To explain why, first observe that we obtained our estimates by separately bounding the spectral norms of the medium and differentiation matrices. Given the definition of the system matrix (Eq. (9)), we expect that our bounds will be sharp if the minimum stepsizes are present in regions where the medium parameters attain their minimum values as well. In practice, this condition is met due to the way the grid is refined. As pointed out in [10], stepsizes should be reduced gradually to avoid large local truncation errors. A consequence of this refinement procedure is that the minimum stepsizes (or stepsizes close to the minimum ones) are present in regions where the medium parameters are small as well, and the upper bounds are therefore expected to be fairly sharp for practical problems.

7. Conclusions

In this paper we have presented explicit and easily computed stability conditions for FDTD on nonuniform tensor product grids. For one-dimensional problems the stability condition is

$$\Delta t < \frac{1}{c_{\max}} \sqrt{\delta_{y;\min} \hat{\delta}_{y;\min}},$$

for two-dimensional problems we have

$$\Delta t < \frac{1}{c_{\max}} \sqrt{\frac{\delta_{x;\min}\hat{\delta}_{x;\min}\delta_{y;\min}\hat{\delta}_{y;\min}}{\delta_{x;\min}\hat{\delta}_{x;\min} + \delta_{y;\min}\hat{\delta}_{y;\min}}},$$

and for three-dimensional problems the stability condition reads

$$\Delta t < \frac{1}{c_{\max}} \frac{1}{\left(\frac{1}{\delta_{x;\min}^2} + \frac{1}{\delta_{y;\min}^2} + \frac{1}{\delta_{z;\min}^2}\right)^{1/4} \left(\frac{1}{\hat{\delta}_{x;\min}^2} + \frac{1}{\hat{\delta}_{y;\min}^2} + \frac{1}{\hat{\delta}_{z;\min}^2}\right)^{1/4}}.$$

All quantities appearing in the upper bounds for the time step are known as soon as the configuration has been specified and discretized. Moreover, for homogeneous media and uniform grids the above conditions simplify to the well-known stability conditions that hold for these particular cases.

References

[1] S. Asvadurov, V.L. Druskin, L. Knizhnerman, Application of the difference Gaussian rules to solution of hyperbolic problems, Journal of Computational Physics 158 (2000) 116–135.
[2] B. Denecker, L. Knockaert, F. Olyslager, D. de Zutter, A new state-space-based algorithm to assess the stability of the finite-difference time-domain method for 3D finite inhomogeneous problems, AEÜ – International Journal of Electronics and Communications 58 (2004) 339–348.
[3] V.L. Druskin, L. Knizhnerman, Gaussian spectral rules for the three-point second differences: I. A two-point positive definite problem in a semi-infinite domain, SIAM Journal on Numerical Analysis 37 (2000) 403–422.
[4] S.D. Gedney, J.A. Roden, Numerical stability of nonorthogonal FDTD methods, IEEE Transactions on Antennas and Propagation 48 (2000) 231–239.
[5] R.B. Lehoucq, D.C. Sorensen, C. Yang, ARPACK Users' Guide: Solution of Large-Scale Eigenvalue Problems with SIAM Publications, SIAM Publications, Philadelphia, PA, 1998.
[6] P. Monk, E. Süli, A convergence analysis of Yee's scheme on nonuniform grids, SIAM Journal on Numerical Analysis 31 (1994) 393–412.
[7] R.F. Remis, On the stability of the finite-difference time-domain method, Journal of Computational Physics 163 (2000) 249–261.
[8] R.F. Remis, Global form of the 2D finite-difference Maxwell system and its symmetry properties, in: Proceedings 2002 IEEE Antennas and Propagation Symposium (June, 2002), San Antonio, pp. 624–627.
[9] R.F. Remis, An implicit time stepping scheme for Maxwell's equations, in: Proceedings of Joint International Conference on Electromagnetics in Advanced Applications (ICEAA'05) and European Electromagnetic Structures Conference (EESC'05), (September, 2005), Torino, pp. 979–982.
[10] A. Taflove, S.C. Hagness, Computational Electrodynamics, the Finite-Difference Time-Domain Method, second ed., Artech House, Norwood, MA, 2000.
[11] S. Wang, F.L. Teixeira, Some remarks on the stability of time-domain electromagnetic simulations, IEEE Transactions on Antennas and Propagation 52 (2004) 895–898.
[12] K.S. Yee, Numerical solution of initial boundary value problems involving Maxwell's equations in isotropic media, IEEE Transactions on Antennas and Propagation 14 (1966) 302–307.